Research Article Vol. 31, No. 5 / 27 Feb 2023 / Optics Express 8170
Optics EXPRESS

Temperature measurements in deployed optical fiber networks using single photon optical time domain reflectometry

THEODOR STAFFAS,* FREDRIK TROIVE, AND VAL ZWILLER

KTH Royal Institute of Technology, Department of Applied Physics, Albanova University Centre, Roslagstullbacken 21, 106 91 Stockholm, Sweden
*tstaffas@kth.se

Abstract: We demonstrate an approach to measure average temperature changes in deployed optical fiber networks using *Optical Time Domain Reflectometry*, OTDR, at the single photon level. In this article we derive a model relating the change in temperature of an optical fiber to the change in time of flight of reflected photons in the fiber in the range $-50 \rightarrow 400$ °C. A setup is constructed to validate this model utilizing a pulsed 1550 nm laser and a *Superconducing Nanowire Single Photon Detector*, SNSPD. With this setup we show that we can measure temperature changes with 0.08 °C accuracy over km distances and we demonstrate temperature measurements in a dark optical fiber network deployed across the Stockholm metropolitan area. This approach will enable in-situ characterization for both quantum and classical optical fiber networks.

1. Introduction

Optical fiber communication is a cornerstone of our daily life in everything from education and entertainment to banking, our continents and seabeds are a spiderweb of optical fiber networks connecting the world [1]. The importance of these communication links necessitates methods to monitor for damage and performance degradation. *Optical Time Domain Reflectometry*, OTDR, is a long-established method to inspect, characterize and certify optical fibers based on analysis of the time of flight of reflected or scattered photons [2] and is used to measure and identify attenuation, faults and bends [3]. There is also much research in using OTDR and other distributed fiber optical sensing techniques to perform measurements in active fiber links for metrology and to utilize a network as a distributed sensor. For example, Giuseppe Marra *et al.* [4] and researchers at Google [5] have shown the potential for monitoring seismic activity on the seabed floor using measurements in fiber networks, or Ming-Fang Huang *et al.* [6] who monitored road traffic using deployed fiber network. These techniques and methods are designed to operate in classical optical fiber networks, such as the ones deployed today, where communication is performed using relatively powerful lasers.

A natural successor or complement to these networks are quantum optical networks where communication is performed by exchanging single photons between nodes [7]. These quantum links are crucial for many proposed applications such as quantum encryption [8,9], quantum random number distribution and synchronization [10], and distributed quantum computing [11,12]. Quantum optical networks also have the same need of monitoring and inspection as classical networks, but a fiber optical sensing technique operating in a quantum network can not rely on powerful laser pulses as this would introduce a high level of interference with a single photon signal. Therefore operation at the single photon level is crucial, and for this we use weak laser pulses and a *Superconducting Nanowire Single Photon Detector*, SNSPD to observe the weak signal. These detectors offer many advantages such as picosecond timing jitter, no after pulsing, low dark count rates and near unity detection efficiency at telecom wavelengths [13–15].

#483404 https://doi.org/10.1364/OE.483404
Journal © 2023 Received 15 Dec 2022; revised 28 Jan 2023; accepted 1 Feb 2023; published 17 Feb 2023

Optics EXPRESS

By utilizing SNSPDs in our system we maximize the range and enable integration with both classical and quantum optical networks to perform single photon OTDR [16,17].

In this paper we build on the trend to utilize the vast deployed fiber networks as sensors and extend the range to quantum networks by using single photon detectors. The time of flight in an optical fiber is not constant and will change due to external factors such as strain, vibration or temperature [6,18]. We present a model that relates the change in the time of flight in an optical fiber to the change of its average temperature. We validate this model experimentally in a laboratory setting and finally demonstrate that our method can be used in a deployed fiber network to monitor temperature changes over long distances and extended time periods. This method enables in-situ monitoring and calibration of quantum fiber links as well as classical optical networks [19].

2. Theoretical background

The time of flight of a photon, τ, to a reflection event in an optical fiber is described by Eq. (1) where L is the fiber distance to the reflection event, n the fiber's effective group index of refraction and c is the speed of light in vacuum.

$$\tau = \frac{2Ln}{c} \tag{1}$$

Both L and n are temperature dependent. Let L_0 be the distance in a fiber at temperature T_0 to a reflection event. If the fiber undergoes a change in temperature to T_1 the distance to the reflection event will change to L_1 due to thermal expansion or contraction. The relation between L_0 and L_1 is determined by the fiber's thermal expansion coefficient α and the change in temperature $\Delta T = T_1 - T_0$ according to Eq. (2).

$$L_1 = L_0(1 + \alpha\Delta T) \tag{2}$$

Similarly, let n_0 and n_1 be the effective group index at temperatures T_0 and T_1. The relation between n_0 and n_1 is determined by the factor $\frac{dn}{dT}$ according to Eq. (3).

$$n_1 = n_0 + \frac{dn}{dT}\Delta T \tag{3}$$

We can now express the time of flight to a reflection event in a fiber at the two different temperatures, T_0 and T_1, as τ_0 and τ_1 by substituting L and n in Eq. (1) by L_0 and n_0, and L_1 and n_1, respectively in Eqs. (4) and (5). We can also use Eqs. (2) and (3) to express τ_1 in terms of L_0 and n_0 in Eq. (5).

$$\tau_0 = \frac{2L_0n_0}{c} \tag{4}$$

$$\tau_1 = \frac{2L_1n_1}{c} = \frac{2L_0n_0}{c}(1 + \alpha\Delta T)(1 + \frac{dn}{dT}\frac{\Delta T}{n_0}) \tag{5}$$

If we assume that ΔT is small and that both α and $\frac{dn}{dT} << 1$ we can ignore the second order term in Eq. (5) and get the first order approximation.

$$\tau_1 = \tau_0(1 + (\alpha + \frac{dn}{dT}\frac{1}{n_0})\Delta T) \tag{6}$$

Using Eqs. (4) and (6) we can express the difference in time of flight, $\Delta\tau$, to a reflection event at temperatures T_0 and T_1. This model assumes a uniform temperature in the fiber between reflection events and can therefore only be used to measure average temperature changes across a fiber.

$$\Delta\tau = \tau_1 - \tau_0 = \tau_0(1 + (\alpha + \frac{dn}{dT}\frac{1}{n_0})\Delta T) - \tau_0 = \tau_0(\alpha + \frac{dn}{dT}\frac{1}{n_0})\Delta T \tag{7}$$

We note that Eq. (7) is dependent on the time of flight at the initial temperature, τ_0. If this temperature is unknown, it is only possible to estimate temperature differences. The two

Optics EXPRESS

material parameters in Eq. (7), α and $\frac{dn}{dT}$, are the thermal expansion coefficient for the silica, $\alpha = 0.55 \times 10^{-6}$ K^{-1}, and $\frac{dn}{dT}$ depends on the doping. Data on this for SMF-28 optical fibers was provided by Proximion AB in the range $-50 \rightarrow 400$ °C, Fig. 1(a). In the region -20 to 60 °C, $\frac{dn}{dT} = 0.8 \times 10^{-5}$ K^{-1}.

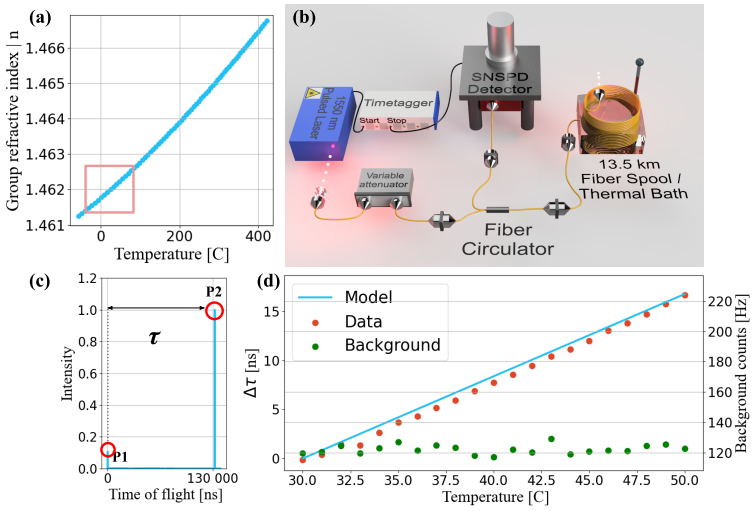

Fig. 1. (a) Group index of refraction, n, of a SMF-28 fiber. The red square indicates the region of interest. In this region the slope is approximately linear by 0.8×10^{-5} K^{-1}; data provided by Proximion AB. (b) Experimental setup to measure change in time of flight vs fiber temperature. A laser diode injects pulses via a circulator into a fiber spool in a thermal bath to control temperature and reflected photons are coupled to an SNSPD. The laser trigger and detection electrical signals are timetagged, allowing us to perform time correlated single photon measurements and extract τ of each photon reflected in the fiber. (c) OTDR measurement of the fiber used in the control experiment. The two peaks are from the fiber ends with the time difference between them used as τ in Eq. (1). (d) Time of flight in a 13.5 km optical fiber while sweeping temperature from 30 to 50 °C. Red dots: measured data. Blue line: modeled line from Eq. (7). Green dots: background noise of the setup, shown to be stable in this temperature region.

3. Experimental setup

To validate the model in Eq. (7), we construct the experimental setup shown in Fig. 1(b). A 1550 nm pulsed laser diode with a repetition rate of 5 kHz generates 70 ps FWHM pulses with spectral bandwidth 0.3 nm that are passed through a variable attenuator to reduce the peak pulse power $<$ 0.15 mW (corresponding to $<$ 82 000 photons / pulse). The pulses are then coupled to a 13.5 km fiber spool placed in a thermal bath. The fiber spool is used for the control experiments and is substituted by a deployed optical fiber network in subsequent measurements.

The photons reflected in the fiber are coupled to an SNSPD with 80% detection efficiency, 19 ps time jitter, $<$ 10 ns dead time, and $<$ 200 Hz dark counts. The laser trigger and detection electrical signals are timetagged with $<$ 9 ps timing jitter. These timetags allow for construction of time of flight histograms, from which the time distance between reflection events are extracted, see Fig. 1. The total timing jitter of the system, ϵ_{sys} is given by Eq. (8), where $\epsilon_{\text{component}}$ is the timing jitter of the individual components. The jitter of the timetagger is counted twice, as it timestamps both the laser sync- and SNSPD detection signal.

$$\epsilon_{\text{sys}} = \sqrt{\Sigma \epsilon^2_{\text{component}}} = \sqrt{19^2 + 9^2 + 9^2}\text{ps} \approx 23\text{ps} \tag{8}$$

Optics EXPRESS

4. Measurements and analysis

4.1. Control experiment

Using the setup in Fig. 1(b) we measure the change in time of flight in the fiber as the temperature is swept from 30 → 50 °C in one degree steps and compare it to our model, Eq. (7), as seen in Fig. 1(c). For every temperature set, the thermal bath was allowed five minutes to reach a stable temperature before three time of flight measurements were performed as well as one measurement of the background signal. The integration time for each measurement was one minute.

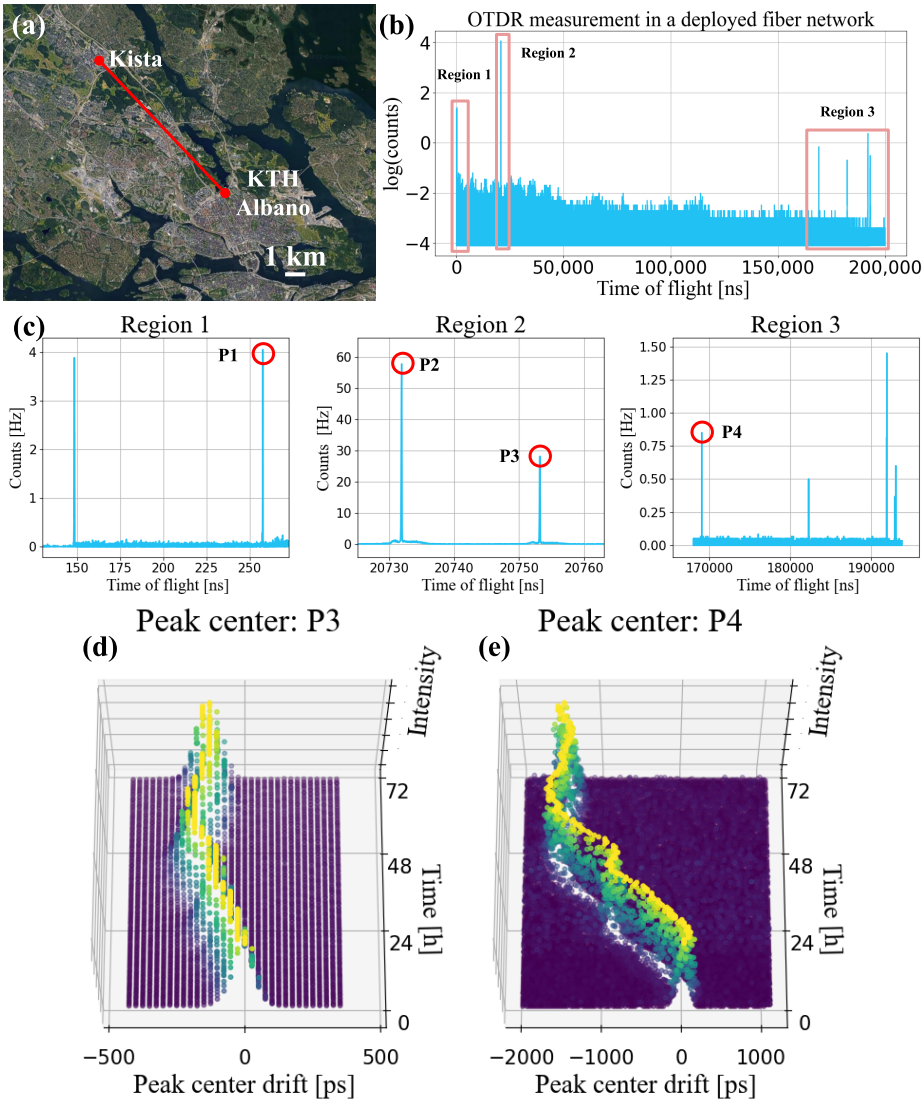

Fig. 2. (a) A map of the nodes of the optical fiber network between KTH and Ericsson in Kista [21] (b) A single OTDR measurement in the fiber network (c) Zoomed in regions of the single OTDR measurement with clear peaks. To track the temperature of the different segments of the optical fiber we measure the change in the distance between P1 as well as P2, and, P3 and P4. (d) and (e) The change in peak center of P3 and P4 respectively over time due to change in temperature.

Optics EXPRESS

For every measurement we construct a time of flight histogram with 25 ps time bins as seen in Fig. 1(c). The bin width was chosen to be slightly larger than the timing jitter of the OTDR setup to smooth out its effects. The time difference between the detector signal and the corresponding laser trigger yields the photon time of flight. This analysis was performed using software optimized to analyze timestamped data [20]. The peaks in the histograms are then identified and the time difference, τ, between subsequent peaks are extracted. An example of the data in a control experiment is shown in Fig. 1(c). The evolution of τ is measured as the temperature is changed and displayed in Fig. 1(d) where τ_0 in Eq. (7) was set as τ at temperature 30 °C. The measured data demonstrates a clear correspondence with our model. The average variation between measurements for a single temperature was 78 ps $\rightarrow$ 0.08 °C and it was noted during the measurements that our temperature controller was stable within 0.3 °C. The background signal of the system, i.e. dark counts from the SNSPD and stray light from the fiber, was measured for each temperature with the laser turned off and shows no evolution as seen by the green dots in Fig. 1(d).

4.2. Deployed fiber network

The setup in Fig. 1(b) was also used to measure the temperature changes in a dark optical fiber network deployed across the Stockholm metropolitan area from the KTH campus at Albano to Ericsson in Kista shown in Fig. 2(a). This fiber network exhibits many more reflection events

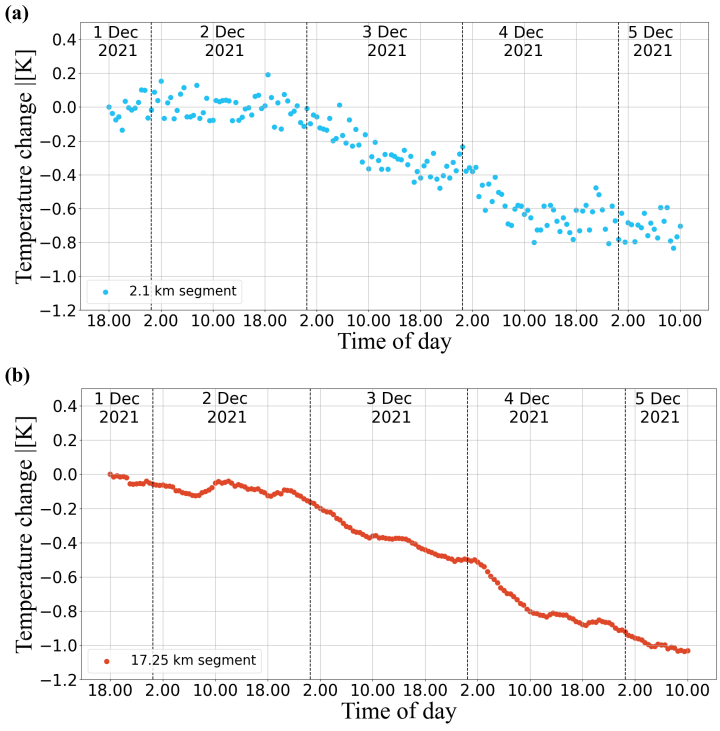

Fig. 3. Measured temperature changes in two segments of a deployed fiber network across the Stockholm metropolitan area over 5 days. (a) Shows the segment between peak 1 and 2 in Fig. 2(c). (b) Shows the segment between peak 3 and 4. Each measurement was performed for 1 minute with 30 minutes intervals. The difference in appearance of the curves in figure (a) and (b) is due to the length of the fiber segments. The segment between peak 3 and 4 is longer, and therefore the temperature curve will appear smoother.

Optics EXPRESS

than the control experiment simply due to the fact that the fiber network consists of multiple fibers and each connection introduces a reflection, displayed in Figs. 2(b) and 2(c). These reflection events correspond to fixed locations along the fiber that can be used as reference points. By tracking the change in time of flight between these reflection events, it is possible to monitor the average temperature change of individual fiber segments.

In Fig. 2(c) four peaks are singled out and 2(d) shows how the centers of two of these peaks shift. We then use the time delay between P1 and P2 as well as P3 and P4 to determine the value of τ for the two respective fiber segments. By monitoring the changes in these values over a period of 88 hours we track the temperature changes the fibers undergo, shown in Figs. 3(a) and 3(b).

5. Conclusion and outlook

In this work we demonstrate a novel approach of monitoring temperature changes in deployed fiber networks using single photon detection events, exploiting the high time resolution, low noise, and single photon sensitivity of SNSPDs. We validate a model for the relation between changes in the time of flight and temperature in an optical fiber and demonstrate measurements in a fiber network across the Stockholm metropolitan area, 17 km between Ericsson in Kista and KTH campus at Albano. By utilizing single photon detectors, this method shows promise for use in quantum networks since these rely on information exchange through single photons. Our system could be installed at the sender and monitor the back reflected signal without interfering with a quantum link. Given that previous works such as Yingqui Mao, et al. [19] have shown the potential of quantum protocols coexisting with classical data traffic in deployed fibers, we see no reason that this method could not be implemented in a classical optical fiber network as well.

In this work we used a pulsed laser at 1550 nm in order to utilize the low signal loss in the optical fiber and to match the maximum detection efficiency of our detectors. A consideration for future implementations would be to instead operate in the O-band to take advantage of the lower dispersion compared to the C-band [22]. We did not observe any noticeable effects of dispersion in our measurement but for implementations in longer networks this might differ. Furthermore, SNSPDs can yield spectral information of the signal [23,24] which could possibly be used to measure Brillouin or Raman scattering.

Acknowledgments. We wish to thank Gunnar Hedin at Proximion AB for sharing their data on fiber temperature dependence as well as Gemma Vall-Llosera and Jonas Almlöf at Ericsson for allowing us to access the deployed fiber network between our lab at KTH and their facility in Kista. Lastly we wish to thank Sabaton for providing ambiance in the lab during measurements.

Disclosures. The authors declare no conflicts of interest.

Data availability. All data sets presented in this work is available upon request.

References

1. T. Horiguchi, "Submarine optical fiber map," https://www.submarinecablemap.com/. Accessed: 2022-12-01.
2. M. Tateda and T. Horiguchi, "Advances in optical time domain reflectometry," J. Lightwave Technol. **7**(8), 1217–1224 (1989).
3. K. Yuksel, M. Wuilpart, V. Moeyaert, and P. Mégret, "Optical frequency domain reflectometry: A review," *ICTON 2009: 11th International Conference on Transparent Optical Networks* pp. 25–29 (2009).
4. G. Marra, C. Clivati, R. Luckett, A. Tampellini, J. Kronjäger, L. Wright, A. Mura, F. Levi, S. Robinson, A. Xuereb, B. Baptie, and D. Calonico, "Ultrastable laser interferometry for earthquake detection with terrestrial and submarine cables," Science **361**(6401), 486–490 (2018).
5. V. Kamalov and M. Cantono, "Using subsea cables to detect earthquakes | google cloud blog," (2020).
6. M. F. Huang, P. Ji, T. Wang, Y. Aono, M. Salemi, Y. Chen, J. Zhao, T. J. Xia, G. A. Wellbrock, Y. K. Huang, G. Milione, and E. Ip, "First field trial of distributed fiber optical sensing and high-speed communication over an operational telecom network," J. Lightwave Technol. **38**(1), 75–81 (2020).
7. D. Lancho, J. Martinez, D. Elkouss, M. Soto, and V. Martin, "Qkd in standard optical telecommunications networks," Lecture Notes of the Institute for Computer Sciences, Social-Informatics and Telecommunications Engineering **36 LNICST**, 142–149 (2010).

Optics EXPRESS

8. J. F. Dynes, A. Wonfor, W. W. Tam, A. W. Sharpe, R. Takahashi, M. Lucamarini, A. Plews, Z. L. Yuan, A. R. Dixon, J. Cho, Y. Tanizawa, J. P. Elbers, H. Greißer, I. H. White, R. V. Penty, and A. J. Shields, "Cambridge quantum network," npj Quantum Inf. **5**(1), 101 (2019).
9. C. Gobby, Z. L. Yuan, and A. J. Shields, "Quantum key distribution over 122 km of standard telecom fiber," Appl. Phys. Lett. **84**(19), 3762–3764 (2004).
10. S. Gyger, K. D. Zeuner, T. Lettner, S. Bensoussan, M. Carlnäs, L. Ekemar, L. Schweickert, C. R. Hedlund, M. Hammar, T. Nilsson, J. Almlöf, S. Steinhauer, G. V. Llosera, and V. Zwiller, "Metropolitan single-photon distribution at 1550 nm for random number generation," Appl. Phys. Lett. **121**(19), 194003 (2022).
11. R. Beals, S. Brierley, O. Gray, A. W. Harrow, S. Kutin, N. Linden, D. Shepherd, and M. Stather, "Efficient distributed quantum computing," Proc. R. Soc. A **469**(2153), 20120686 (2013).
12. A. S. Cacciapuoti, M. Caleffi, F. Tafuri, F. S. Cataliotti, S. Gherardini, and G. Bianchi, "Quantum internet: Networking challenges in distributed quantum computing," IEEE Network **34**(1), 137–143 (2020).
13. C. M. Natarajan, M. G. Tanner, and R. H. Hadfield, "Superconducting nanowire single-photon detectors: Physics and applications," Supercond. Sci. Technol. **25**(6), 063001 (2012).
14. J. Chang, J. W. Los, J. O. Tenorio-Pearl, N. Noordzij, R. Gourgues, A. Guardiani, J. R. Zichi, S. F. Pereira, H. P. Urbach, V. Zwiller, S. N. Dorenbos, and I. E. Zadeh, "Detecting telecom single photons with 99.5 - 2.07 + 0.5 % system detection efficiency and high time resolution," APL Photonics **6**(3), 036114 (2021).
15. D. V. Reddy, S. W. N. Richard, P. Mirin Robert, R. Nerem, and V. B. Verma, "Superconducting nanowire single-photon detectors with 98 system detection efficiency at 1550 nm," Optica **7**(12), 1649 (2020).
16. Q. Zhao, L. Xia, C. Wan, J. Hu, T. Jia, M. Gu, L. Zhang, L. Kang, J. Chen, X. Zhang, and P. Wu, "Long-haul and high-resolution optical time domain reflectometry using superconducting nanowire single-photon detectors," Sci. Rep. **5**(1), 10441 (2015).
17. P. Eraerds, M. Legré, J. Zhang, H. Zbinden, and N. Gisin, "Photon counting otdr: advantages and limitations," J. Lightwave Technol. **28**(6), 952–964 (2010).
18. J. K. Yang, A. J. Kerman, E. A. Dauler, B. Cord, V. Anant, R. J. Molnar, and K. K. Berggren, "Suppressed critical current in superconducting nanowire single-photon detectors with high fill-factors," IEEE Trans. Appl. Supercond. **19**(3), 318–322 (2009).
19. Y. Mao, B.-X. Wang, C. Zhao, G. Wang, R. Wang, H. Wang, F. Zhou, J. Nie, Q. Chen, Y. Zhao, Q. Zhang, J. Zhang, T.-Y. Chen, and J.-W. Pan, "Integrating quantum key distribution with classical communications in backbone fiber network," Opt. Express **26**(5), 6010–6020 (2018).
20. Z. Lin, L. Schweickert, S. Gyger, K. Jöns, and V. Zwiller, "Efficient and versatile toolbox for analysis of time-tagged measurements," J. Instrum. **16**(08), T08016 (2021).
21. "Map of stockholm," https://www.google.com/maps. Accessed: 2022-10-01.
22. "Corning smf-28," https://www.corning.com/media/worldwide/coc/documents/Fiber/SMF-28%20ULL.pdf. Accessed: 2022-12-11.
23. E. Reiger, S. Dorenbos, V. Zwiller, A. Korneev, G. Chulkova, I. Milostnaya, O. Minaeva, G. Gol'tsman, J. Kitaygorsky, D. Pan, W. Slysz, A. Jukna, and R. Sobolewski, "Spectroscopy with nanostructured superconducting single photon detectors," IEEE J. Select. Topics Quantum Electron. **13**(4), 934–943 (2007).
24. L. Kong, Q. Zhao, H. Wang, J. Guo, H. Lu, H. Hao, S. Guo, X. Tu, L. Zhang, X. Jia, L. Kang, X. Wu, J. Chen, and P. Wu, "Single-detector spectrometer using a superconducting nanowire," Nano Lett. **21**(22), 9625–9632 (2021).